BNL-65222

59

CONF-980117--

Non-thermal photodesorption of N_2 from Ag (111)

R. M. Rao, R. J. Beuhler and M. G. White

Chemistry Department, Brookhaven National Laboratory, Upton, NY 11973

ABSTRACT

We have measured translational and rotational energy distributions of N_2 molecules following desorption from a Ag(111) surface by infrared (1064 nm) radiation. The observed desorption yields were large even at laser fluences far below that required for laser-induced thermal desorption. State-resolved laser techniques using coherent VUV radiation showed that the rotational and translational energy distributions of the desorbing N_2 molecules are not consistent with the predictions of the heat diffusion model governing laser-induced surface heating. These results suggest that physisorbed adsorbates can couple directly to the nascent-phonon distribution or the nascent electron-hole pairs in the photoexcited substrate without heating of the surface.

Keywords : photodesorption, state-selective detection, nitrogen, Ag (111)

1. INTRODUCTION

Photon stimulated desorption (PSD) of physisorbed species can proceed via three different mechanisms[1], depending on where the photon energy is deposited. The deposition of the photon energy directly to the adsorbate-substrate bond can desorb the adsorbate by direct excitation from its vibrational ground state to continuum translational states.[2-5] Resonant excitation of an internal molecular vibration of the adsorbate by the photon can lead to transfer of energy to the surface bond and its subsequent release from the surface.[6-8] In general, for non-resonant excitations[9], the photons are absorbed by the solid, where substrate excitations couple to the surface bond and thus lead to desorption. In this study, we shall present results of infrared-induced desorption of physisorbed N_2 on Ag (111), where the photon energy is far from threshold (no direct excitation of N_2-Ag bond), and is not resonant with intra-molecular vibrations. The expectation is that substrate excitations lead to desorption of N_2 from the silver surface.

In this work, we present the results of state-resolved measurements of infrared (IR) induced desorption of physisorbed N_2 on Ag (111). These studies are an extension of previous work on CO/Ag (111) where we observed non-thermal desorption dynamics for photoexcitation with near-IR (1064 nm) and visible (532 nm) laser light.[9] Specifically, the translational and rotational "temperatures" of the desorbed CO molecules were found to be well described by Boltzmann distributions, but they did not exhibit any power dependence over a factor of 3200 in IR fluence. The lack of power dependence over such a wide range in IR power is inconsistent with that expected for a laser-induced thermal desorption process. Furthermore, the desorption yields were found to scale approximately linearly with IR fluence instead of exponentially for thermally driven desorption following Arrhenius kinetics. These

DISCLAIMER

surprising results suggest a non-thermal desorption mechanism, yet the low energy photons (1.16 eV) and weak electronic interactions between $CO_{(a)}$ and the Ag substrate make the conventional DIET models appear improbable. To gain further insight into the non-thermal IR desorption process, similar experiments were performed for physisorbed N_2 including power dependence of the rotational and translational energies. Unlike in the CO work, however, variable temperature studies were also performed which revealed a strong temperature dependence to the onset of IR-induced desorption. The latter suggests that the IR laser alone cannot induce desorption without some initial vibrational excitation of the low frequency N_2-Ag bond.

2. EXPERIMENTAL

The apparatus used in these experiments is shown schematically in Fig.1. Its main features are a windowless VUV generation chamber, an open-cycle liquid helium (LHe) cooled sample manipulator and a differentially-pumped, time-of-flight (TOF) mass spectrometer. The apparatus has been described in detail elsewhere[10] and only a brief discussion of the experiments presented here will be given.

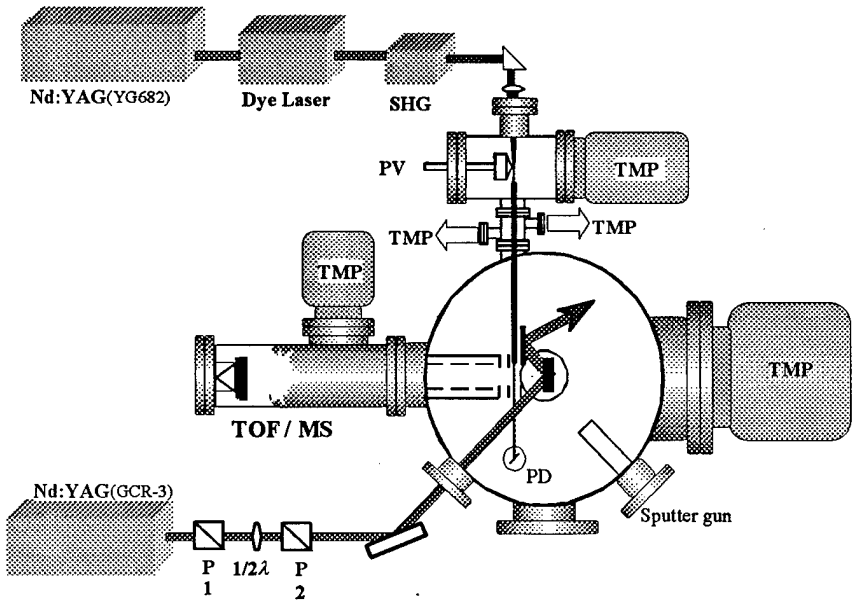

Figure 1: Schematic of the surface photochemistry apparatus.
TMP: turbomolecular pump
P: polarizer
PD: platinum photodiode
PV: pulsed valve
TOF-MS: time-of-flight mass spectrometer.

The substrate used in these experiments was a commercially obtained 12.7 mm diameter and 2 mm thick Ag (111) crystal (Monocrystals). The electropolished, oriented Ag (111) single crystal was mounted at the bottom of a rotatable, LHe cooled cryostat. Monolayer coverages of molecular nitrogen on silver were achieved by back filling the chamber to the appropriate pressure for 10 L exposures. The 10L exposure used in this work was determined by coverage dependent thermal desorption spectroscopy (TDS) and the detection of multilayer formation which desorbs at a distinctly lower temperature (34 K) than the monolayer (38 K).

A pulsed Nd:YAG laser (Quanta-Ray GCR3, 20 Hz) was used to generate the infrared (1064 nm) radiation for desorption of N_2. A Glan-Thompson prism polarizer (Lambrecht) and 1/2λ plate were used to establish p-polarized light relative to the crystal surface and a second polarizer was used for setting the incident power. The collimated IR or UV laser beam was apertured to a 0.7 cm (dia.) spot incident on the crystal at 45°. Reflected radiation from the crystal is directed away from the interaction region of the spectrometer by a small gold mirror mounted on the back of the first ion extraction electrode (see Fig. 1).

The coherent VUV radiation required for (1+1′) REMPI detection of N_2 via the $b^1\Pi_u \leftarrow X^1\Sigma_g^+$ (1,0) transition (98.5 to 98.6 nm)[11-13] was produced via non-resonant third harmonic generation ($\omega_{vuv} = 3\omega_{uv}$) in a free jet expansion Ar gas.[14] Tunable UV (295.5 to 295.8 nm) laser light for VUV generation was produced by a Nd:YAG pumped dye laser system (Spectra-Physics GCR-230 (20Hz), Laser Analytics LDL 20505 dye laser) followed by second harmonic generation in an angle-tuned KDP crystal. The UV beam was focused into a chamber with synchronously pulsed, expanding free jet of argon gas. The harmonically generated VUV radiation and the diverging fundamental UV beams are captured by a capillary light guide and directed from the VUV chamber to the surface chamber. Two stages of differential pumping provide a pressure differential of about 10^8 across the capillary light guide, thus permitting UHV conditions to be routinely maintained within the surface chamber. The VUV and UV beams are used to state-selectively excite and photoionize, respectively, the desorbed N_2 molecules, which are then accelerated into the TOF mass spectrometer and detected by a dual microchannel plate array. The distance from the crystal surface to the VUV laser beam is 2.5 cm and that defines the neutral flight path for velocity measurements of the desorbed species. The delay between the desorption laser and the VUV probe laser is scanned to derive the arrival time distribution of the desorbing molecules

As noted above, the photodesorbed N_2 molecules are detected by (1+1′) REMPI via excitation to the $b^1\Pi_u$, $v'' = 1$ state. Assuming that the ionization rate is limited by the one-photon excitation step driven by the relatively weak VUV radiation, rotational state populations can be derived by dividing the intensity of the REMPI signal by the rotational line strength factor $S_{JJ''}$ (including nuclear spin statistics for N_2).[15] Previous studies of the $b^1\Pi_u$ state, however, have shown this state to be predissociative,[11-13] with line intensities not quite matching the calculated line strengths.[13] In an effort to obtain effective line strength factors which could be applied to an unknown ground state distribution, e.g. desorbed molecules, (VUV+UV) REMPI measurements were performed on a thermalized, room temperature sample. The sensitivity of this ionization scheme permits such measurements to be performed at a background pressures as low as 10^{-8} Torr. Using the known ground state rotational constant B'' (= 2.010 cm^{-1})[16] and assuming a Boltzmann rotational distribution at 300 K, the appropriate scale factors ($Sc_{JJ''}$) were determined for each rotational branch transition (P, Q, R) in the place of the rotational line strength factors ($S_{JJ''}$). The experimentally generated scale factors were used to extract rotational state populations in this work and will be published elsewhere.[17]

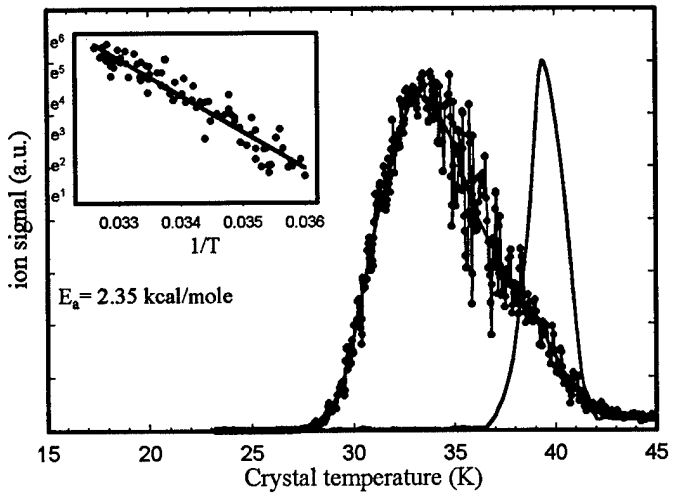

Figure 2: Comparison of N_2 thermal desorption spectra (TDS) from a Ag(111) surface taken with (data points) and without (line) exposure to IR radiation. The IR fluence was 93 μJ/cm^2. Desorbed N_2 in the v″=0, J″=4 quantum state was detected by (1+1′) REMPI detection via the b←X transition. The delay between the IR and probe lasers was set at 70 μsec corresponding to the maximum of the arrival-time-distribution of N_2 molecules. The inset shows the low temperature onset region of the IR-TDS curve from which an apparent activation energy of 2.4 kcal/mole can be extracted. The activation energy for the conventional TDS curve is determined to be 6 kcal/mole.

3. RESULTS

In Fig. 2 we compare TDS curves taken for monolayer coverages of N_2 dosed at a surface temperature of 23 K with and without exposure to the IR laser. The heating rates are 0.15 K/sec and the signal was obtained by (1+1′) REMPI detection of N_2 in the $X^1\Sigma_g^+$, v″=0, J″= 4 quantum state. The delay between the desorption and probe lasers was set to 70 μsec which corresponds to the maximum in the time-of-flight arrival distribution for the N_2 molecules (see figure 4). The conventional TDS curve is very sharp (~2 K FWHM) with a desorption temperature of 39 K and an activation energy of 6 kcal assuming zero-order desorption kinetics. By contrast, the TDS curve taken during IR irradiation (referred to hereafter as an IR-TDS curve) is much broader with a shifted peak maximum and

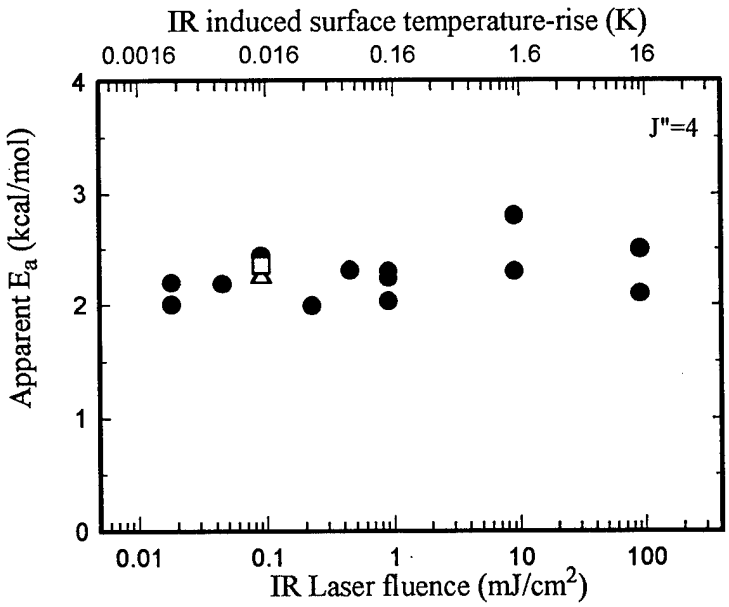

Figure 3: Apparent activation energies extracted from IR-TDS curves as a function of laser fluence. Shown on the top axis is the calculated surface temperature rise induced by the IR laser (see text for details).

Probe laser delay: ● 70 μs △ 50 μs □ 125 μs

substantially lower desorption temperature onset. The pulse energy density (fluence) of the IR radiation incident on the crystal was 93 $\mu J/cm^2$. More significantly, the leading edge of the IR-TDS curve exhibits a well-behaved exponential rise, which can be used to obtain an apparent activation energy as shown in the inset of Fig. 2. The latter is substantially lower (2.4 kcal) than for thermal desorption and suggests that the IR photoexcitation provides an additional source of energy to facilitate desorption at a lower temperature. Similar experiments were performed for a wide range of IR pulse energies, the results of which are shown in Fig 3. Surprisingly, the apparent activation energies exhibit no power dependence, though the IR-TDS desorption onset temperatures vary between 23 K (lower limit of crystal temperature) at high fluences (>100 mJ/cm^2) and 29 K at the lowest fluence (19 $\mu J/cm^2$).

As a result of the strong temperature dependence discussed above, it was necessary to carefully control the surface temperature for performing measurements of the translational and rotational state distributions of the desorbed N_2 molecules. In particular, the IR-induced desorption rates become very rapid at surface temperatures above 30-32 K (depending on laser fluence) so that the N_2 monolayer is essentially removed before the measurements can be completed. These so-called depletion rates are determined under the same conditions of IR laser power and surface temperature by measuring the desorption yield as a function of laser exposure. Typical state-resolved measurements for a surface

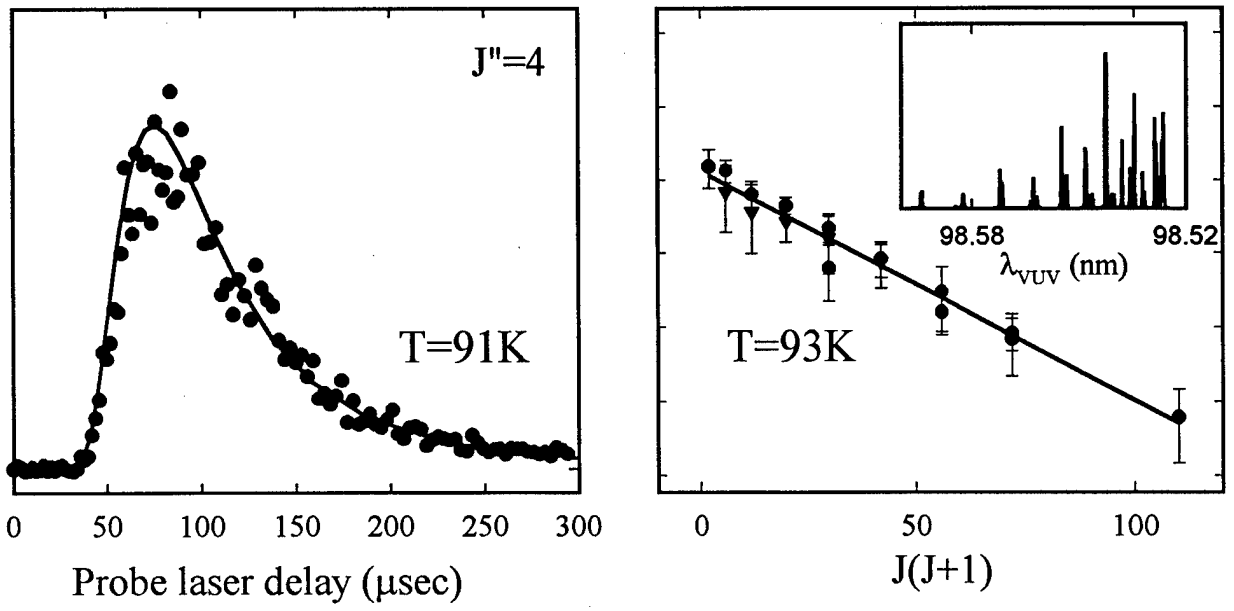

Figure 4: State-resolved measurements for IR-induced desorption of N_2 from Ag(111) surface at 29 K and a IR-laser fluence of 93 $\mu J/cm^2$. The left panel gives the arrival-time-distribution of N_2 molecules in the v"=0, J"=4 quantum state measured by varying the flux-weighted Boltzmann velocity distribution at 91 K converted to time-of-flight for comparison to the data. The right panel contains rotational state populations extracted from the b←X (1+1') REMPI spectrum (shown as insert) for a fixed arrival-time (velocity) of 70 μsec. The data are plotted as ln(pop J") versus J"(J"+1) and the straight line regression yields a rotational temperature of 93 ± 10 K.

temperature of 29 K and IR fluence of 93 μJ/cm^2 are shown in Figure 4, including the corrections for the depletion rate. The arrival-time distribution for N_2 molecules in the v″=0, J″=4 quantum state is shown in the upper curve and is consistent with a Boltzmann velocity distribution (solid line) with an average translational energy ($\langle E_t \rangle/2k$) of 91 K. This translational "temperature" is well above that of the surface (29 K) even including the infinitesimally small increase due to IR-induced surface heating (< 0.1 K). The latter is estimated from the classical heat diffusion model[18] using published thermal[19] and optical constants[20] of Ag metal. The rotational state distribution is shown in the lower curve of Fig. 4 as determined by measurements of the (1+1′) $b^1\Pi_u \leftarrow X^1\Sigma_g^+$ (1,0) REMPI spectrum and derived populations using the experimentally determined scale factors ($Sc_{JJ''}$) discussed above. The rotational distribution is also found to conform to Boltzmann statistics with a characteristic temperature (93 K) that is essentially identical to the observed translational temperature. These results imply equilibration of the translational and rotational degrees of freedom, but at energies representative of the desorption process and not the surface temperature. This equilibration may reflect the weak anisotropy of the N_2-Ag (111) potential which may show little preference for the N-N bond direction, particularly in the excited transition state prior to desorption.

In Figure 5, we show the measured average translational energies as a function of IR laser fluence at a fixed surface temperature of 29 K. Despite a factor of 200 in power variation, the average translational energy only changes by about 25 % over the same range. Furthermore, the data at 93 μJ/cm^2 indicates a small (negative) correlation between average translational energy and rotational quantum state. This weak dependence of final state energy on IR fluence is similar to that found in our earlier work on CO/Ag (111) where the translational *and* rotational energies were followed as a function of IR power.[9] In that work, the data were taken at a surface temperature (42 K) chosen to eliminate the possibility of multilayer formation and just happened to be fortuitously close to the IR-TDS onset temperature where the cross section for IR-induced desorption is significant. Consequently, the

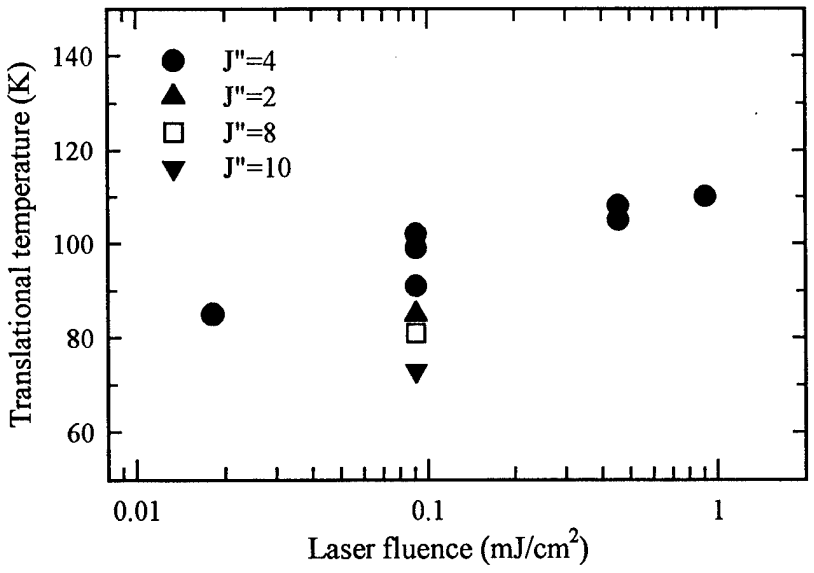

Figure 5: Average translational energies $\langle E_t \rangle/2k$ derived from measured arrival-time-distributions as a function of IR fluence and rotational quantum state.

important role of surface temperature in the IR-induced desorption process (see Fig. 2) was not known.

In general, the lack of strong power dependencies in the N_2 final state energies and apparent IR-TPD activation energies clearly point to a non-thermal desorption process.[21] Although not shown here, the depletion rates for IR-induced desorption at fixed temperature are also found to vary linearly with IR fluence rather than the expected exponential increase for a laser-induced thermal process following Arrhenius kinetics.[21, 22] The observation of a temperature onset for the IR-induced process, *i.e.*, the IR-TDS curves such as Fig. 2, further shows that the IR-driven desorption process requires

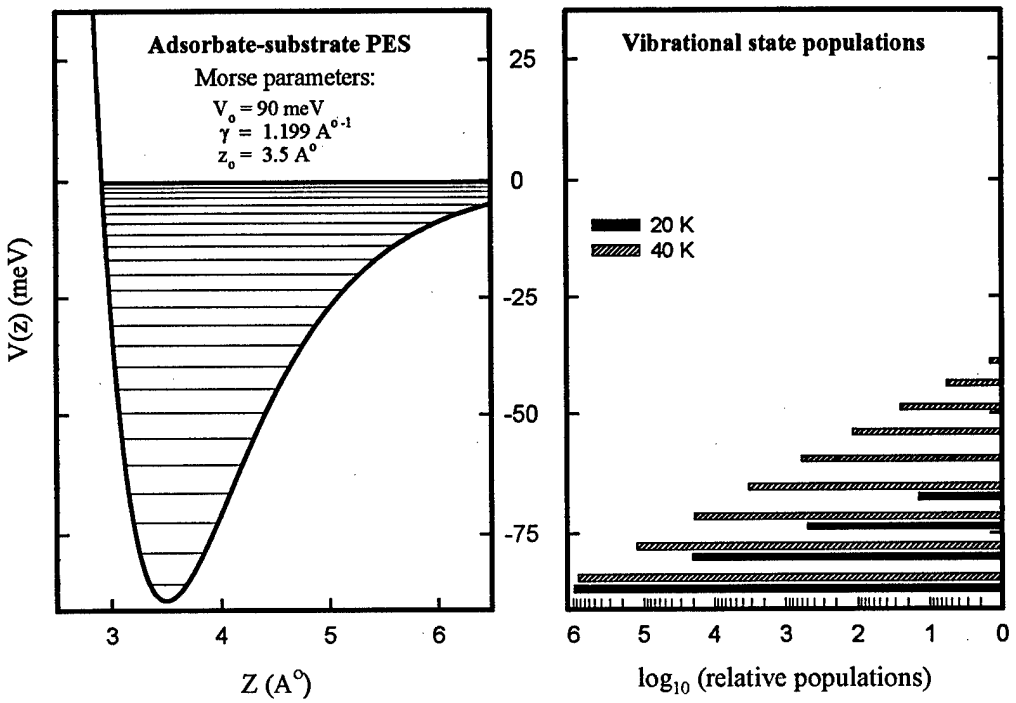

Figure 6: Calculated Morse potential for the N_2-Ag(111) stretch vibration (left panel) and vibrational populations for 20 K and 40 K (right panel.

thermal excitation of the adsorbate-substrate system. The latter is most likely indicative of vibrational excitation of the very low frequency center-of-mass motions (molecule-surface vibration, frustrated rotation and translation). The thermal population of the very high frequency N-N internal vibration (ω_e = 2358 cm^{-1}) [16] would be essentially unaffected at the low surface temperatures covered by the IR-TDS curves. The most relevant center-of-mass motion to desorption is the N_2-Ag stretch. In Figure 6, we show a parameterized Morse potential, $V_0[1 - e^{-2\gamma (z - z_0)}]$, for the N_2 - Ag (111) stretch as determined from theoretical studies of N_2 – Ag scattering,[23] in an effort to indicate the change in vibrational state distribution as a function of surface temperature. The Morse parameters are V_0 = 90 meV (well depth), γ = 1.199 $Å^{-1}$ (range) and z_0 = 3.5 Å (equilibrium separation) and a vibrational frequency of $\omega_e \sim$ 150 cm^{-1}. The relative vibrational populations are shown in the right panel of Fig. 6 for temperatures of 20 K and 40 K. Although the absolute change in the population of the v = 0 level does not change

significantly (~15 %), the populations of levels with $v \geq 2$ increase by orders of magnitude from 20 K to 40 K. The role of the IR photoexcitation is to provide a pathway for these vibrationally excited adsorbate-substrate complexes to reach the dissociative continuum. Likely scenarios include non-adiabatic interactions between nascent electron-hole pairs and the N_2 - Ag stretch motion, or vibrational ladder climbing transitions induced by interactions with a non-thermalized distribution of lattice phonons produced by electron/hole scattering. Although non-adiabatic interactions between electron-hole pairs and center-of-mass motions have been invoked in femtosecond laser excitation experiments, these applications typically involve chemisorbed systems, *e.g.* CO on Cu,[25,26,28] where non-adiabatic interactions are mediated by the strong electronic interactions between the adsorbate and substrate. For physisorbed systems, such electronically mediated interactions are less likely, so that vibrational ladder climbing induced by laser-excited lattice phonons appears as the most promising mechanism. Clearly, the excited phonon distribution responsible for the IR-induced desorption is non-thermal, since the laser-induced heating even at the highest IR fluences used in this work is negligibly small. Tests of this mechanism, however, will require the extension of current microscopic descriptions of thermal desorption,[29] which explicitly treat phonon-induced vibrational transition probabilities, to non-equilibrium systems.

5. ACKNOWLEDGEMENTS

This work was performed at Brookhaven National Laboratory and supported by the US Department of Energy, Office of Basic Energy under contract No. DE-AC02-76CH00016.

4. REFERENCES

1. H. J. Kreuzer and Z. W. Gortel, *Physisorption Kinetics*, Springer Series in Surface Science Vol. 1 (Springer, Berlin, 1986).
2. M. S. Slutsky and T. F. George, *Chem. Phys. Lett.* **57**, 474 (1978).
3. J. Lin and T. F. George, *Chem. Phys. Lett.* **66**, 5 (1979).
4. C. Jedrzejek, K. F. Freed, S. Efrima, and H. Metiu, *Surf. Sci.* **109**, 191 (1981).
5. K. A. Pearlstine and G. M. McClelland, *Surf. Sci.* **134**, 389 (1983).
6. D. Lucas and G. E. Ewing, *Chem. Phys.* **58**, 385 (1981).
7. T. J. Chuang and H. Seki, *Phys. Rev. Lett.* **49**, 382 (1982).
8. I. Hussla, H. Seki, T. J. Chuang, Z. W. Gortel, H. J. Kreuzer, and P. Piercy, *Phys. Rev. B* **32**, 3489 (1985).
9. L. Fleck, R. J. Beuhler, and M. G. White, *J. Chem. Phys.* **106**, 3813 (1997).
10. R. Rao, J. Dvorak, R. J. Beuhler and M. G. White, to be published.
11. P. K. Carroll and C. P. Collins, Can. J. Phys. **47**, 563 (1969).
12. D. Stahel, M. Leoni, and K Dressler, J. Chem. Phys. **79**, 2541 (1983).
13. W. Ubachs, L. Tashiro, and R. N. Zare, Chem. Phys. **130**, 1 (1989).

14. R. H. Page, R. J. Larkin, A. H. Kung, Y. R. Shen and Y. T. Lee, *Rev. Sci. Instrum.* **58**, 1616 (1987).
15. G. Herzberg, *Molecular Spectra and Molecular Structure: I. Spectra of Diatomic Molecules* (Van Nostrand, New York, 1950), p. 208.
16. K. P. Huber and G. Herzberg, *Molecular Spectra and Molecular Structure: IV. Constants of Diatomic Molecules* (van Nostrand, New York, 1979).
17. R. Rao, R. J. Beuhler and M. G. White, to be published.
18. J. M. Hicks, in *Laser Spectroscopy and Photochemistry on Surfaces*, Part I, H.-L. Dai and W. Ho, editors (World Scientific, Singapore, 1995), p. 589 and references therein.
19. C. Y. Ho, R. W. Powell and P. E. Liley, *J. Phys. Chem. Ref. Data* **1**, 279 (1972); C. Y. Ho, R. W. Howell and K. Y. Wu, *Proceedings on the 8th Conference on Thermal Conductivity*, edited by C. Y. Ho and R. E. Tayler (Plenum, New York, 1969), p. 971.
20. J. H. Weaver, *et al., in Optical Properties of Metals, edited by H. Behrens and G. Ebel (Fachinformationszentrum, Karlsruhe, 1981).*
21. J. P. Cowin, D. J. Auerbach, C. Becker, and L. Wharton, *Surf. Sci.* **78**, 545 (1978); I. Hussla, H. Coufal, F. Träger, and T. J. Chuang, *Can. J. Phys.* **64**, 1070 (1986); D. Burgess, Jr., R. R. Cavanagh, and D. S. King, *J. Chem. Phys.* **88**, 6556 (1988).
22. D. Burgess, Jr., P. C. Stair and E. Weitz, *J. Vac. Sci. Technol.* **A4**, 1362 (1986); J. L. Brand and S. M. George, *Surf. Sci.* **167**, 341 (1986); Z. Rosenweig and M. Asscher, *J. Chem. Phys.*, **96**, 4040 (1992).
23. J. C. Tully, C. W. Muhlhausen and L. R. Ruby, *Ber. Bunsenges. Phys. Chem.* **86**, 433 (1982); C. W. Muhlhausen, J. A. Serri, J. C. Tully, G. E. Becker and M. J. Caedillo, *Israel J. Chem.* **22**, 315 (1982).
24. J. A. Misewich, T. F. Heinz, P. Wiegand and A. Kalamarides, in *Laser Spectroscopy and Photochemistry on Surfaces*, Part II, H.-L. Dai and W. Ho, editors (World Scientific, Singapore, 1995), p. 764 and references therein.
25. C. Springer and H. Head-Gordon, *Chem. Phys.* **205**, 73 (1996); J. C. Tully, M. Gomez and M. Head-Gordon, *J. Vac Sci. Technol.* **A 11**, 1914 (1993); M. Head-Gordon and J. C. Tully, *J. Chem. Phys.* **96**, 3939 (1992).
26. J. P. Culver, M. Li, Z.-J. Sun, R. M. Hochstrasser and A. G. Yodh, *Chem. Phys.* **205**, 159 (1996); J. P. Culver, M. Li, L. G. Jahn, R. M. Hochstrasser and A. G. Yodh, *Chem. Phys. Lett.* **214**, 431(1993).
27. H. Aizawa and S. Tsuneyuki, *Surf. Sci.* **377**, 610 (1997).
28. L. M. Sruck, L. J. Ritter, S. A. Buntin, R. R. Cavanagh and J. C. Stephenson, *Phys. Rev. Lett.* **77**, 4576 (1996).
29. for example see: S. Efrima, C. Jedrzejek, K. F. Freed, E. Hood and H. Metiu, *J. Chem. Phys.* **79**, 2436 (1983); C. Jedrzejek, K. F. Freed, S. Efrima and H. Metiu, *Chem. Phys. Lett.* **79**, 227 (1981).

Report Number (14) BNL--65222
CONF-980117--

Publ. Date (11) 199802
Sponsor Code (18) DOE/ER, XF
UC Category (19) UC-401, DOE/ER

DOE